of ice in supercooled clouds at temperatures below about –10 or –20°C. It has already been established that contrails affect the atmosphere primarily at temperatures below –40°C (*15*). This process extends the envelope for aircraft effects on the atmosphere to warmer temperatures. Inadvertent seeding may not be important globally, but regionally near major airports in midlatitudes during cool weather months it may lead to enhanced precipitation at the ground. Polar clouds are particularly susceptible to the effect, modifying incoming and outgoing radiative fluxes near the surface and therefore local meteorology and climatology.

References and Notes

1. V. C. Schumacher, *Z. Angew. Met.* **57**, 214 (1940).
2. *Weather* **3**, 232 (1948).
3. *Weatherwise* **21**, 1 (1968).
4. A. L. Rangno, P. V. Hobbs, *J. Clim. Appl. Meteorol.* **22**, 214 (1983).
5. A. L. Rangno, P. V. Hobbs, *J. Clim. Appl. Meteorol.* **23**, 985 (1984).
6. K. Gierens, B. Kärcher, H. Mannstein, B. Mayer, *J. Atmos. Sci.* **66**, 217 (2009).
7. A. J. Heymsfield *et al.*, *Bull. Am. Meteorol. Soc.* **91**, 753 (2010).
8. R. S. Sekhon, R. C. Srivastava, *J. Atmos. Sci.* **27**, 299 (1970).
9. The selection of candidate aircraft is available as supporting material on *Science* Online, together with a table detailing aircraft types and numbers.
10. W. C. Skamarock, J. B. Klemp, *J. Comput. Phys.* **227**, 3465 (2008).
11. G. Thompson, P. R. Field, R. M. Rasmussen, W. D. Hall, *Mon. Weather Rev.* **136**, 5095 (2008).
12. W. L. Woodley *et al.*, *J. Appl. Meteorol.* **42**, 640 (2003).
13. The method of quantification is available as supporting material on *Science* Online.
14. D. Zhang, Z. Wang, D. Liu, *J. Geophys. Res.* **115**, D00H13 (2010).
15. H. Appleman, *Bull. Am. Meteorol. Soc.* **34**, 14 (1953).

16. The authors wish to thank contributors to the data used in this study: N. Mirsky, N. Downs, E. Zrubek, M. Carmody, B. Skamarock, J. Tuttle, P. Kennedy, C. Velden, D. Spangenberg, and J. Robaidek. Editing by M. Miller and graphics with particular help from A. Norton, co-developer of VAPOR software, are greatly appreciated. This research was supported by the National Center for Atmospheric Research through NSF, through NASA from grants NNX07AQ85G and NNX10AN18G, and through the FAA Aviation Climate Change Research Initiative.

Supporting Online Material

www.sciencemag.org/cgi/content/full/333/6038/77/DC1
Materials and Methods
Figs. S1 to S3
Table S1

13 January 2011; accepted 19 May 2011
10.1126/science.1202851

Pattern in Escalations in Insurgent and Terrorist Activity

Neil Johnson,[1] Spencer Carran,[2,3] Joel Botner,[4] Kyle Fontaine,[5] Nathan Laxague,[1] Philip Nuetzel,[5] Jessica Turnley,[6] Brian Tivnan[7,8]

In military planning, it is important to be able to estimate not only the number of fatalities but how often attacks that result in fatalities will take place. We uncovered a simple dynamical pattern that may be used to estimate the escalation rate and timing of fatal attacks. The time difference between fatal attacks by insurgent groups within individual provinces in both Afghanistan and Iraq, and by terrorist groups operating worldwide, gives a potent indicator of the later pace of lethal activity.

In 1948, Lewis Fry Richardson found that the number of wars with a given number of fatalities follows an approximate power-law statistical distribution as a function of the number of fatalities (*1*). Recent research has shown that a similar statistical distribution arises for the number of fatalities in individual clashes and acts of terrorism (*2*, *3*), whereas the relative stability of these distributions over time allows an estimate to be given of the severity of future wars or clashes within an ongoing war (*2*–*4*). However, these existing studies say nothing about the operationally relevant questions (*5*–*7*) of how the underlying arms race evolves over time, or when fatal attacks might occur. Here, we confront these questions using fatality data obtained on an unprecedented daily scale from the ongoing insurgent war in Afghanistan and the recent one in Iraq. Our data analysis is freely available for public scrutiny: The coalition military fatality data come from the public Web site www.icasualties.org. Our analysis was done with the free downloadable tool Open Office, which runs on any computer platform. The supporting online material (SOM) for this paper contains step-by-step instructions together with Open Office worksheets. For Afghanistan, we include fatalities from the start of Operation Enduring Freedom in 2001 until summer 2010, when General Petraeus became commander of the International Security Assistance Force and the U.S.-led surge started. For Operation Iraqi Freedom, the data include fatalities from 2003 until summer 2010, when U.S. military action officially ended. The terrorism results are derived from a recent study, which used the database of the Memorial Institute for the Prevention of Terrorism, comprising the 3143 fatal attacks carried out by the 381 known terrorist groups operating within the period 1968–2008 (*8*). Suicide bombing data for Hezbollah (1982–1985) and Pakistan militants (1995–2008) comes from the public Web site http://cpost.uchicago.edu.

For a wide range of human activities, the time taken to complete a given challenging task decreases with successive repetitions, following an approximate power-law progress curve (*8*–*12*). This inspires us to analyze the insurgents' completion of fatal attacks against coalition military forces in a similar way (Fig. 1, A and B). We calculated the best-fit power-law progress curve $\tau_n = \tau_1 n^{-b}$, where τ_n represents the interval between the $(n-1)$'th and n'th fatal day (one in which the insurgent activity produces at least one coalition military death), where $n = 1, 2, 3$, etc. b indicates the escalation rate. τ_1 is the time interval between the first 2 days with coalition military fatalities. (For global terrorism, a fatal day is one in which a particular terrorist group produced at least one death anywhere in the world.) Figure 1C shows the best-fit values τ_1 and b for each province in Afghanistan, for all forms of hostile death. The average number of fatalities per fatal attack is fairly constant in a conflict (*2*, *3*, *8*), hence it is in insurgents' interest (or that of a particular terrorist group) that the time between fatal days decrease rapidly, and hence b is large and positive, while the opposite is true for the military (or counterterrorism force). The scatter in τ_n in Fig. 1B is typical for real-world tasks (in particular, given the ongoing two-way struggle), and the Pearson rank product-moment correlation coefficient (R^2) is within an acceptable range for social systems (*9*–*14*). Although alternative progress curve forms are possible, any such two-parameter progress curve amounts to a nonlinear transformation of the power-law form and hence generates a more complex version of Fig. 1C. An exponential form does not generate systematically better progress-curve fits; R^2 for the power-law form is better by up to 70% for three-quarters of the provinces, including (most importantly) those with the most data points, and only tends to be comparable for the few provinces having sparse datapoints and larger τ_n scatter. We do not consider events with no deaths because they occur almost daily; moreover, the injury statistics are not publicly available. Although the data resolution time scale is 1 day, this is not problematic, because the τ_n values dictating the best-fit progress curve for a given province, or terrorist group, are usually much larger than 1.

Figure 1C reveals a surprising linear relationship between the best-fit progress curve values τ_1 and b for individual provinces. The straight line through the provinces has $R^2 = 0.9$ and is given by the equation $b = m\log_{10}\tau_1 + c$, with best-fit parameter values $m = 0.89$ and $c = -1.22$. Even if one speculated that the τ_1 and b values have to lie somewhere in this range (which, a priori,

[1]Department of Physics, University of Miami, Coral Gables, FL 33124, USA. [2]Department of Biology, University of Miami, Coral Gables, FL 33124, USA. [3]Department of Mathematics, University of Miami, Coral Gables, FL 33124, USA. [4]Department of Computer Science, University of Miami, Coral Gables, FL 33124, USA. [5]Department of International Studies, University of Miami, Coral Gables, FL 33124, USA. [6]Galisteo Consulting Group, Albuquerque, NM 87110, USA. [7]The MITRE Corporation, McLean, VA 22102, USA. [8]Complex Systems Center, University of Vermont, Burlington, VT 05405, USA.

they do not), a simple Monte Carlo calculation puts the probability of this linear relationship emerging by chance with a comparable R^2 at less than 1 in 10^6. Figure 2 shows that the linear relationship extends to a specific weapon [that is, fatalities caused by improvised explosive devices (IEDs)] and to a completely different insurgent conflict (Iraq), as well as to global terrorism and suicide bombings by individual groups. These τ_1 and b values suggest, for example, that common organizational processes underlie all hostile military fatalities in Farah and Kunar, IED military fatalities in Kabul, and fatal terrorist attacks. The fact that Fig. 2 shows larger scatter than Fig. 1C is understandable given its inclusion of events in separate countries and the sparser number of IED fatalities as compared to total hostile fatalities. Although the Afghanistan provinces exhibit an escalation of fatal days throughout the entire data set (that is, decreasing τ_n), the Iraq provinces cease to show pure escalation toward the end of the conflict, where fatalities cease. Because this paper focuses on escalation, the Iraq data points in Fig. 2 correspond to the initial escalation up to the turning point in the cumulative moving average of τ_n. Other reasonable methods for determining a turning point retain the same linear structure as that in Fig. 2.

We considered the possibility that these results derive from contagion or diffusion effects due to proximity. The data points for Kandahar, Kunar, and Farah sit nearby in Fig. 1C, showing that their escalation patterns are almost identical; however, they are widely separated geographically within Afghanistan, with Kandahar in the south, Kunar in the east, and Farah in the west. If fatal days in different provinces were synchronized in calendar time (which they are not), they would sit at the same point in Fig. 1C, but they do not. Likewise, if fatal days in different provinces were independent, then the individual (τ_1, b) points should be scattered randomly across Fig. 1C, but they are not. Comparing Fig. 1C to detailed sociotechnical maps (*15*), we could not detect a clear systematic relationship between the data point locations and effects such as proximity to Pakistan, density of internally displaced persons, common tribal warlords, or levels of poppy production (*16*). In terms of increases in troop or insurgent numbers, it would have required a very complex and specific province-dependent increase, combined with a very contrived mathematical relationship to fatalities, to produce the observed patterns. Instead, the calendar times for the n'th fatal day vary wildly between provinces (for instance, the first recorded military fatality in Paktia was 4 March 2002, whereas in Wardak it was 25 July 2007). Nor are the observed patterns simply linked to an increase in the number of troops and hence to an increase in the number of targets, because monthly troop increases in Afghanistan were almost linear, not a power curve (*16*, *17*). Furthermore, as observed in Iraq after the surge, significant troop increases can actually decrease the military fatality rate.

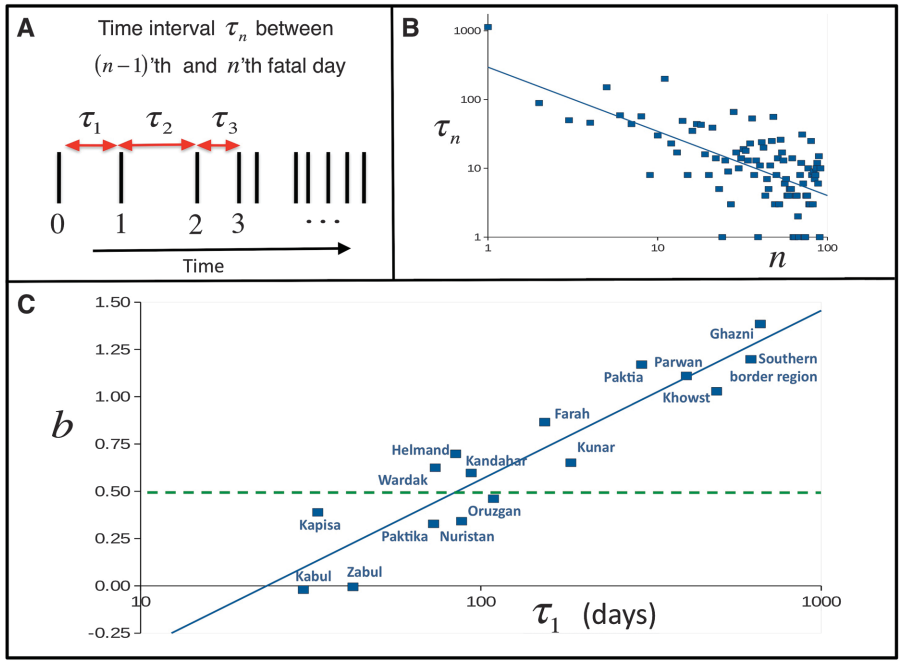

Fig. 1. (**A**) Schematic timeline of successive fatal days shown as vertical bars. τ_1 is the time interval between the first two fatal days, labeled 0 and 1. (**B**) Successive time intervals τ_n between days with IED fatalities in the Afghanistan province of Kandahar (squares). On this log-log plot, the best-fit power-law progress curve is by definition a straight (blue) line with slope $-b$ (b is an escalation rate). (**C**) The solid blue line shows best linear fit through progress-curve parameter values τ_1 and b for individual Afghanistan provinces (blue squares) for all hostile fatalities (all coalition military fatalities attributed to insurgent activity). The green dashed line shows value $b = 0.5$, which is the situation in which there are no correlations. The subset of fatalities recorded in icasualties as "southern Afghanistan" is shown as a separate region because of their likely connection to operations near the Pakistan border.

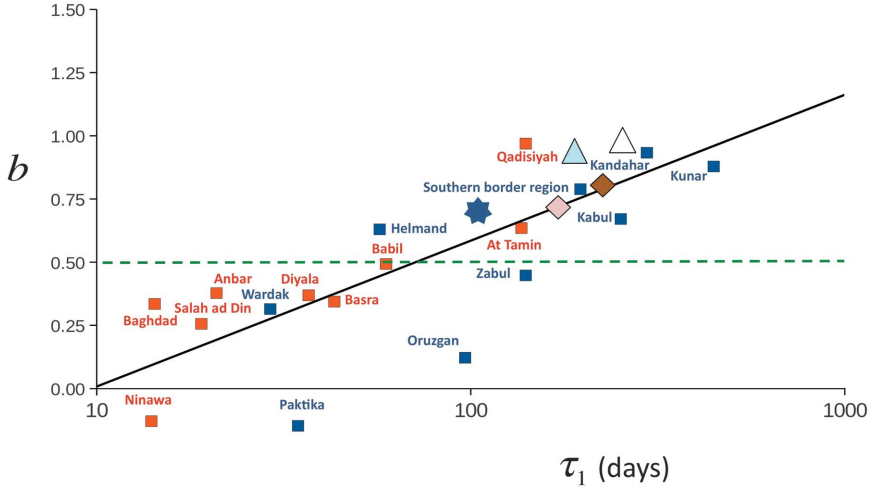

Fig. 2. The solid black line shows the best linear fit through progress-curve parameter values τ_1 and b for IED fatalities in provinces in Afghanistan (blue squares) and Iraq (red squares). Because the frequency of IED fatalities for provinces sitting just below $b = 0$ is low, their b values are relatively uncertain and should be regarded simply as $b \approx 0$. The green dashed line is at $b = 0.5$. These findings are consistent with results for IED data aggregated over all Afghanistan (blue star) and for global terrorism and suicide bombings. Global terrorism: The dark diamond shows the τ_1 and b values deduced from the best-fit progress curve for global terrorist group activity when averaged over all attacks (*8*); the light diamond is an alternative estimate where τ_1 and b are calculated directly by inserting the time intervals between initial attacks into the progress curve formula (SOM). Suicide bombings: The blue triangle is for Hezbollah suicide attacks, and the white triangle is for suicide attacks within Pakistan (data are from http://cpost.uchicago.edu/).

We also analyzed timelines from detailed online reports concerning political events (SOM); however, these timelines represented a poor fit to a progress curve ($R^2 = 0.2$) and produced (τ_1, b) values ($\tau_1 = 12.4$ and $b = -0.75$), which were unlike those shown in Figs. 1C or 2.

Our broad-brush theory does not require knowledge of specific adaptation or counteradaptation mechanisms, and hence bypasses issues such as changes in insurgent membership, technology, learning, or skill set, as well as a need to know the hearts and minds of local residents. We regard the escalation of hostilities as representing adaptation and counteradaptation in a way that is analogous to the Red Queen hypothesis of evolutionary biology (*18*, *19*). The traditional story features the Red Queen (which in our context is an insurgency, or terrorist group) running as fast as she can just to stay at the same place, implying that her Blue King opponent (the coalition military or antiterrorism organization) instantaneously and perfectly counteradapts to her advances so that they are always neck and neck (the distance between the two $R = 0$). However, instantaneous and perfect counteradaptation is unrealistic; indeed, complex adaptation-counteradaptation dynamics generated by sporadic changes in circumstances imply that R's temporal evolution is likely to be so complex that it can be modeled as a stochastic process (*20*, *21*). We do not need to know exactly why R changes at any specific moment, nor do the changes in R have to have the same value, because each change is the net result of a mix of factors [such as learning by experience or changes in personnel and technology (*5*–*7*)] for each opponent. When the Red Queen is in the lead ($R > 0$), there will inevitably be fatal days. If her lead increases, the rate of fatal days should also increase, hence for $R > 0$, we take the instantaneous rate of fatal days as proportional to R. As R tends to 0, fatal days become increasingly rare. When $R < 0$, the Blue King holds the lead and there are no fatal days. By definition, provinces with no fatal days do not appear in Figs. 1C and 2 (mathematically, τ_1 becomes infinite and b is undefined). The provinces in Figs. 1C and 2 exhibit escalation and are therefore consistent with an R that is generally positive and increasing over time. For these provinces, significant changes in the Red Queen's lead R are likely to occur around fatal days, making R a function of n: The Red Queen has by definition become successful at that moment and this may stimulate a further increase in R, whereas the Blue King's failure may stimulate an effective counteradaptation effort and hence reduce R. In the simple limiting case where changes in R are statistically independent and have finite variance, the Central Limit Theorem (*20*) says that the typical magnitude (the root mean square) of the Red Queen's lead R after n steps varies as n^b, where $b = 0.5$ (SOM), which is the random walk result widely used in physics, biology, and economics (*20*–*22*). For the more general and realistic case in which changes in R depend on prior history, research on correlated walks shows that b will deviate from 0.5 but will typically remain in the range $0 \leq b \leq 1.5$ (*20*–*22*), in agreement with Figs. 1C and 2. Because the rate is inversely proportional to the time interval, this gives $\tau_n = an^{-b}$, where a is a constant of proportionality. Setting $n = 1$ yields $\tau_1 = a$, hence our theory reproduces the empirical finding that the escalation of fatal days follows an approximate power-law progress curve $\tau_n = \tau_1 n^{-b}$ with typical values in the range $0 \leq b \leq 1.5$. Our theory interprets provinces with b values near 1 as having an ineffective military counteradaptation, so that R persistently increases at every step n, hence $R \propto n^b$ with $b = 1$. This is analogous to the Red Queen moving steadily forward at constant velocity while the Blue King remains stuck at the starting line. If the Red Queen gains momentum, R can start accelerating and hence $b > 1$ as observed for some provinces such as Paktia and Ghazni in Fig. 1C. The fact that b values for IEDs appear to be concentrated between 0 and 1 (Fig. 2) whereas the all-hostile range is from 0 to 1.5 (Fig. 1C) suggests that the coalition military counteradapts to IEDs better than to other threats. Provinces at $b = 0$ (Kabul and Zabul in Fig. 1C) have a constant rate of fatal days, implying that the military is managing to contain further escalation. Similar interpretations can be made for any other data point in Figs. 1C and 2, according to its b value.

The linear relationship between τ_1 and b in Figs. 1C and 2 can be reproduced by adding a coupling between the Red Queen–Blue King arms races in different provinces. This coupling can arise for various reasons: Even though the insurgent groups (Red Queens) operating in two different locations may be unconnected, and even though they inflict military fatalities at different points in space and calendar time, the Blue King opponent is essentially the same for each (the same military coalition), and hence the insurgents in one province may eventually adopt successful tactics from another. On the Blue King side, the widespread use of similar tactics or equipment could generate coupling. For example when MRAPs (Mine Resistant Ambush Protected vehicles) were moved to Afghanistan, the Blue King effectively took on very similar operational characteristics in each country: slow, lumbering movement restricted to certain transport corridors.

To illustrate the potential of our findings, suppose that a quiet region suddenly experiences 2 fatal days. We can estimate the escalation rate b for future fatal days in that region by taking the initial time interval to be τ_1 and reading off the corresponding b value from Fig. 1C or 2. An estimate for the date of the m'th future fatal day can also be obtained by summing all time intervals $n < m$ using $\tau_n = \tau_1 n^{-b}$. Figure 1B suggests that actual time intervals may exhibit significant scatter around the τ_n estimates; however, their sum (and hence the actual calendar date) will show less variability because positive and negative errors in τ_n tend to cancel when summed. Inputting only the first data point in Fig. 1B, the error between the predicted and actual time of the ultimate fatal day ($n = 92$, which occurred on 13 May 2010) is less than 25%, which is far smaller than the scatter in individual τ_n values might have suggested. Access to detailed classified data sets would enable future analysis to fully explore this possibility, and may help establish a systematic approach to quantifying an insurgency's momentum, the effectiveness of countermeasures, and that of countermeasure training processes. The fact that Figs. 1C and 2 link progress curves across two current theaters of war and global terrorism may open broader lines of inquiry into group learning, adaptive management strategies, and production metrics associated with modern uprisings, such as those underway in the Middle East. One might argue that analyses of this kind are useless once publicly known, because they can be invalidated by insurgents' free will. However, we believe this will not happen for the same reason that all commuters know that a traffic jam will appear every day at rush hour on a certain route, yet many still end up joining it. External constraints of working hours, school schedules, and finite numbers of direct roads mean that such predictability is hard to avoid. Similarly, the spontaneity of fatal attacks by an insurgency is probably constrained by many factors, including the availability of troop convoys, explosive materials, and sympathy within the local population.

References and Notes

1. L. F. Richardson, *J. Am. Stat. Assoc.* **43**, 523 (1948).
2. J. C. Bohorquez, S. Gourley, A. R. Dixon, M. Spagat, N. F. Johnson, *Nature* **462**, 911 (2009).
3. A. Clauset, M. Young, K. S. Gleditsch, *J. Conflict Resolut.* **51**, 58 (2007).
4. M. Lim, R. Metzler, Y. Bar-Yam, *Science* **317**, 1540 (2007).
5. M. T. Flynn, *Fixing Intel: A Blueprint for Making Intelligence Relevant in Afghanistan* (Center for a New American Security, Washington, DC, 2010).
6. J. Robb, *Brave New War: The Next Stage of Terrorism and the End of Globalization* (Wiley, Hoboken, NJ, 2007).
7. D. Kilcullen, *The Accidental Guerrilla: Fighting Small Wars in the Midst of a Big One* (Oxford Univ. Press, Oxford, 2009).
8. A. Clauset, K. S. Gleditsch, e-print available at http://arxiv.org/abs/0906.3287v1 (2009).
9. J. M. Dutton, A. Thomas, *Acad. Manage. Rev.* **9**, 235 (1984).
10. L. Argote, D. Epple, *Science* **247**, 920 (1990).
11. S. P. Saraswat, J. T. Gorgone, *Inf. Manage.* **19**, 53 (1990).
12. A. Mottrie *et al.*, *Eur. Urol.* **58**, 127 (2010).
13. N. Ducheneaut *et al.*, in *Proceedings of CHI 2007*, Special Interest Group on Computer-Human Interaction, 28 April to 3 May 2007, San Jose, CA (Association for Computing Machinery Press, New York, 2007).
14. J. Cohen, *Statistical Power Analysis for the Behavioral Sciences* (Lawrence Erlbaum Associates, Hillsdale, NJ, ed. 2, 1988).
15. www.nps.edu/programs/ccs/index.html.
16. A. Belasco, *Troop Levels in the Afghan and Iraq Wars*, 7-5700, R40682 (Congressional Research Service, Washington DC, 2009).
17. International Security Assistance Force, ISAF Troop Numbers 2008–2010, 14 January 2011; as referred to in (*23*).

18. D. D. P. Johnson, *J. Wash. Acad. Sci.* **95**, 89 (2009).
19. R. D. Sagarin *et al.*, *Nature* **465**, 292 (2010).
20. J. Rudnick, G. Gaspari, *Elements of the Random Walk* (Cambridge Univ. Press, Cambridge, 2010)
21. D. Ben-Avraham, S. Havlin, *Diffusion and Reactions in Fractals and Disordered Systems* (Cambridge Univ. Press, Cambridge, 2000)
22. N. F. Johnson, P. Jefferies, P. M. Hui, *Financial Market Complexity* (Oxford Univ. Press, Oxford, 2003), p. 20.
23. J. Bohannon. *Science* **331**, 1256 (2011).

Acknowledgments: The authors gratefully acknowledge support for this research from the Joint IED Defeat Organization, IDN# N70465, and from The MITRE Corporation and the Santa Fe Institute for their co-hosting of the "Mathematics of Terrorism" workshop. The views and conclusions contained in this paper are those of the authors and should not be interpreted as representing the official policies, either expressed or implied, of any of the above named organizations, to include the U.S. government. We also thank P. Dodds, C. Danforth and A. Clauset for broad discussions surrounding this topic, L. Amaral for discussions concerning non-Poissonian behavior, and the anonymous reviewers for suggestions.

Supporting Online Material
www.sciencemag.org/cgi/content/full/333/6038/81/DC1
SOM Text
Figs. S1 to S3
SOM Data Analysis

2 March 2011; accepted 26 May 2011
10.1126/science.1205068

Mechanism of RAD51-Dependent DNA Interstrand Cross-Link Repair

David T. Long,[1] Markus Räschle,[2] Vladimir Joukov,[3] Johannes C. Walter[1]*

DNA interstrand cross-links (ICLs) are toxic DNA lesions whose repair in S phase of eukaryotic cells is incompletely understood. In *Xenopus* egg extracts, ICL repair is initiated when two replication forks converge on the lesion. Dual incisions then create a DNA double-strand break (DSB) in one sister chromatid, whereas lesion bypass restores the other sister. We report that the broken sister chromatid is repaired via RAD51-dependent strand invasion into the regenerated sister. Recombination acts downstream of FANCI-FANCD2, yet RAD51 binds ICL-stalled replication forks independently of FANCI-FANCD2 and before DSB formation. Our results elucidate the functional link between the Fanconi anemia pathway and the recombination machinery during ICL repair. In addition, they demonstrate the complete repair of a DSB via homologous recombination in vitro.

In vertebrate cells, DNA interstrand cross-link (ICL) repair is coupled to DNA replication and involves structure-specific endonucleases, translesion DNA polymerases, recombinases, and numerous proteins mutated in the human disease Fanconi anemia (FA) (*1*). FA is characterized by genomic instability and cellular sensitivity to DNA interstrand cross-linking agents. A central event in the FA pathway is the ubiquitylation of the FANCI-FANCD2 heterodimer, which activates it for ICL repair (*2*, *3*). Extensive evidence indicates that homologous recombination (HR) is essential for ICL repair (*4*–*9*). However, the precise role of HR in ICL repair remains conjectural, and the functional connection between the FA and HR pathways is unclear.

Using *Xenopus* egg extracts, we established a cell-free system for replication-dependent repair of a plasmid containing a single, site-specific cisplatin ICL (pICL) (Fig. 1A) (*2*, *10*). Upon addition of pICL to egg extracts, replication initiates at a random site, and two replication forks converge on the ICL (Fig. 1B, i). The leading strand of one fork is then extended to within one nucleotide of the ICL (Fig. 1B, ii). Next, dual incisions surrounding the ICL create a DNA double-strand break (DSB) in one sister chromatid, and translesion DNA synthesis restores the other sister by first inserting a nucleotide across from the adducted base (Fig. 1B, iii), followed by strand extension beyond the ICL (Fig. 1B, iv). Ultimately, 5 to 25% of replicated pICL is fully repaired, as measured by regeneration of a SapI site that was originally interrupted by the cross-link (*2*, *10*). In the absence of ubiquitylated FANCD2, DNA incisions, lesion bypass, and SapI site regeneration are greatly diminished (*2*). Given the established links between HR and ICL repair and the inefficient removal of the unhooked ICL in egg extracts (*10*), we postulated that SapI site regen-

[1]Department of Biological Chemistry and Molecular Pharmacology, Harvard Medical School, Boston, MA 02115, USA. [2]Department of Proteomics and Signal Transduction, Max Planck Institute of Biochemistry, 82152 Martinsried, Germany. [3]Department of Cancer Biology, Dana-Farber Cancer Institute, Boston, MA 02115, USA.

*To whom correspondence should be addressed. E-mail: johannes_walter@hms.harvard.edu

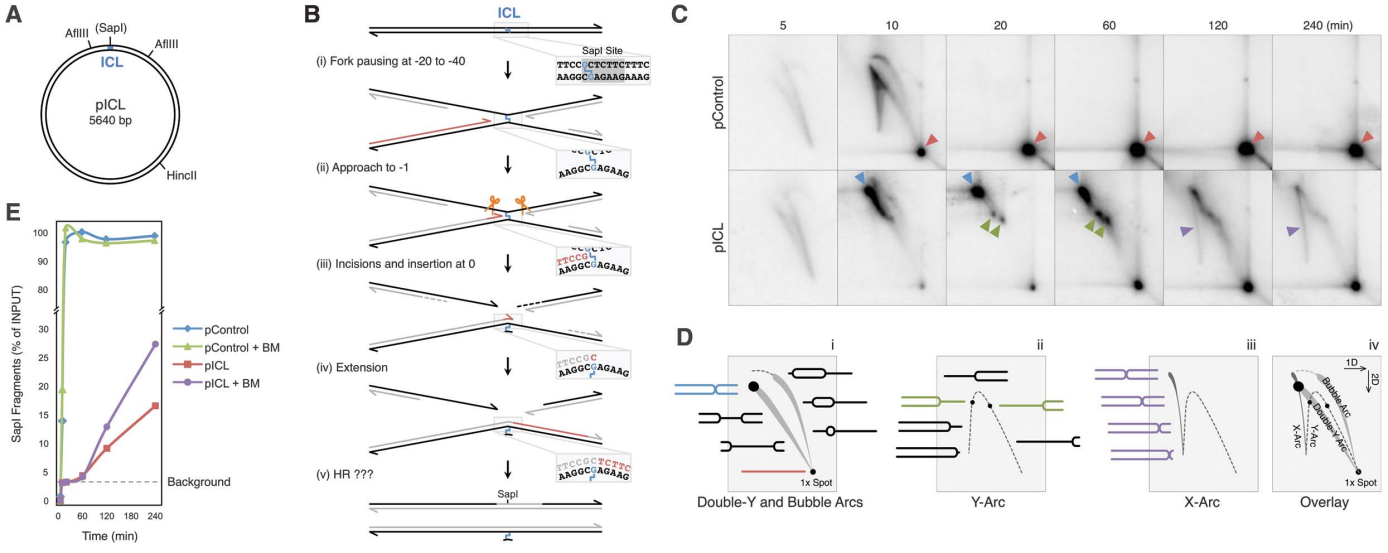

Fig. 1. The X-arc contains intermediates of ICL repair. (**A**) pICL schematic. (**B**) Model of ICL repair in *Xenopus* egg extracts (*2*, *10*). (**C**) pControl or pICL was replicated in egg extract, digested with HincII, and analyzed by 2DGE. Arrowheads, see main text. (**D**) Cartoon of 2DGE patterns and relevant DNA intermediates. (**E**) ICL repair of samples from (C) was analyzed under normal and branch migration (+BM) conditions. Background, SapI fragments from contaminating un–cross-linked plasmid. For primary data, see fig. S1, E and F. All graphed experiments were performed at least three times, and a representative example is shown.